

# Rapid #: -14597615

CROSS REF ID: **1110458**

LENDER: **LHL4CRLRM :: Main Library**

BORROWER: **ORE :: Main Library**

TYPE: Article CC:CCL

JOURNAL TITLE: International journal of vehicle systems modelling and testing

USER JOURNAL TITLE: International journal of vehicle systems modelling and testing

ARTICLE TITLE: Prediction of rolling resistance and steering characteristics using finite element analysis truck tyre model

ARTICLE AUTHOR: Rustam Ali; Ranvir Dhillon; Moustafa El-Gindy; Fre

VOLUME: 8

ISSUE: 2

MONTH:

YEAR: 2013

PAGES: 179-

ISSN: 1745-6436

OCLC #:

Processed by RapidX: 4/12/2019 1:15:49 PM



This material may be protected by copyright law (Title 17 U.S. Code)

---

## Prediction of rolling resistance and steering characteristics using finite element analysis truck tyre model

---

Rustum Ali, Ranvir Dhillon and  
Moustafa El-Gindy\*

Faculty of Engineering and Applied Science,  
UOIT, 2000 Simcoe Street N,  
Oshawa, ON, L1K 7K4, Canada  
E-mail: rustam.ali@mycampus.uoit.ca  
E-mail: ranvir.dhillon@uoit.ca  
E-mail: moustafa.el-gindy@uoit.ca

\*Corresponding author

Fredrik Öijer and Inge Johanson

Volvo Group Trucks Technology,  
Chassis Strategies and Vehicle Analysis Department,  
26661, AB4S, 405 08 Göteborg, Sweden  
E-mail: Fredrik.Oijer@volvo.com  
E-mail: Inge.S.Johansson@volvo.com

Mukesh Trivedi

Volvo Group Trucks Technology,  
Features, Verification and Validation America,  
7900 National Service Rd.,  
Greensboro, NC 27409, USA  
E-mail: mukesh\_trivedi@yahoo.com

**Abstract:** The purpose of this research is to provide insight into the design and development of a finite element analysis (FEA) model of a heavy truck tyre for the purpose of investigating rolling resistance and steering characteristics. Aspects considered include the effects of design parameters (tyre dimensions, construction, materials, and FEA modelling technique) and operating parameters (tyre inflation pressure, vehicle speed, spindle load, and road surface texture). The model was also developed to predict the effects of combined steering and camber angles on cornering forces, aligning and overturning moments. The findings of this investigation show that the multi-layer membrane material can accurately simulate the tyre carcass structure. Validation tests include the static load-deflection test and dynamic cleat-drum excitation test. The experimental data shows that the generated FEA tyre and wheel model qualitatively simulates a real heavy truck radial tyre. Further work is required to allow for accurate quantitative prediction and would vary largely with tyre construction.

**Keywords:** finite element analysis; FEA; truck tyre; tyre mechanics; rolling resistance; slip and camber angles; steering characteristics; simulation; modelling.

**Reference** to this paper should be made as follows: Ali, R., Dhillon, R., El-Gindy, M., Öijer, F., Johanson, I. and Trivedi, M. (2013) 'Prediction of rolling resistance and steering characteristics using finite element analysis truck tyre model', *Int. J. Vehicle Systems Modelling and Testing*, Vol. 8, No. 2, pp.179–201.

**Biographical notes:** Rustam Ali is alumni and Research Assistant at the University of Ontario Institute of Technology in the Faculty of Engineering and Applied Science.

Ranvir Dhillon is a graduate student at the University of Ontario Institute of Technology in the Faculty of Engineering and Applied Science.

Moustafa El-Gindy is an Associate Professor at the University of Ontario Institute of Technology in the Faculty of Engineering and Applied Science.

Fredrik Öijer holds an MSc in Mechanical Engineering from Chalmers University of Technology and is a Senior Technology Specialist in Vehicle Analysis-Durability at Volvo GTT.

Inge Johanson holds an MSc in Mechanical Engineering from Chalmers University of Technology and is Group Manager in Vehicle Analysis at Volvo GTT.

Mukesh Trivedi is a former Senior Engineer at Volvo Group Trucks Technology-Features, Verification and Validation America.

## 1 Introduction

A heavy truck tyre experiences extreme loads for prolonged periods and is a key component of the heavy truck. Due to the large extent that modern society relies on transport, tyre dynamics and fuel efficiency make a large impact on traffic safety, environmental pollutants and fuel expenses.

Two major industry standards are used for the measurement of rolling resistance of tyres. The SAE and ISO standards are used for experimental data collection, which is then further processed to eliminate external influences and obtain comparable, uniform data.

The test equipment used for both these tests is a drum-spindle machine, which consists of a large drum on which the tyre rolls, and a spindle, to which the test tyre is mounted. The spindle lowers down until the tyre makes contact with the drum, and the position of the spindle may be locked in respect to the distance from the drum, to simulate a large load which may cause deflection of the tyre sidewall.

The SAE recommends the use of one of three methods to measure rolling resistance of pneumatic tyres. The recommendations apply to passenger car, light truck, highway truck and bus tyres. SAE document J1269 (2000) provides a standard method for gathering data on a uniform basis so as to allow easy comparison and evaluation. Similar

to SAE recommended practices for measuring rolling resistance, the ISO lists methods of measuring rolling resistance in document ISO 28580:2009 (2009). The methods use a similar approach to obtain data.

### 1.1 Rolling resistance prediction

Previous research into the rolling resistance of tyres has been extensive; some prominent literature on the subject is presented in Wong (2008) and other publications such as Dukkipati et al. (2008) and Pacejka (2006). According to Wong, the rolling resistance of tyres on hard surfaces is primarily caused by the hysteresis in tyre materials due to the deflection of the carcass while rolling. In addition to internal hysteresis, friction between the tyre and the road caused by sliding, the resistance due to air circulating inside the tyre, and the fan effect of the rotating tyre on the surrounding air are secondary sources of rolling resistance.

Wong (2008) presented models capable of estimating the rolling resistance coefficient of a truck tyre at speed up to 100 km/h and tyre pressure ranging between 90–120 psi as follows:

- for a radial-ply truck tyre:  $f_r = 0.006 + 0.23 \times 10^{-6} \times V^2$
- for a bias-ply truck tyre:  $f_r = 0.007 + 0.45 \times 10^{-6} \times V^2$

where  $f_r$  is the rolling resistance force in Newtons and  $V$  is the velocity of the vehicle in kilometres per hour.

Rakah et al. (2001) also cite a truck rolling resistance model described in Fitch (1994). It is presented as a linear function based on the vehicle speed and mass, with consideration of road surface material and condition:

$$R_r = 9.8066C_r (c_2V + c_3) \frac{M}{1,000}$$

where  $M$  is the total mass,  $C_r$  is the rolling coefficient of the surface, and  $c_2$  and  $c_3$  are coefficients for radial or bias-ply tyres.

In a free-rolling tyre, when there is no applied wheel torque, the rolling resistance is a longitudinal force present between the tyre and ground contact patch. Wong (2008), as well as Dukkipati et al. (2008), defined the ratio of the rolling resistance to the normal load on the tyre as the coefficient of rolling resistance:

$$C_r = \frac{f_x}{f_z}$$

where  $C_r$  represents the coefficient of rolling resistance,  $f_x$  is rolling resistance force and  $f_z$  is the vertical (normal) force at the tyre-ground contact patch.

## 2 FEA tyre modelling

There has been a considerable amount of work on the development and validation of FEA tyre models for various purposes. Some research into the rolling resistance prediction of rolling tyres is available; however it is limited due to the high amounts of computing

power required for accurate prediction. Furthermore, the limitations of the FEA method are apparent when validating the models developed through various tests. Chae et al. (2006) presented an early simplified tyre and results of some static and dynamic simulations including contact patch area, vertical stiffness, first mode of free vertical vibration and yaw oscillation frequency. Allen et al. (2007) developed simplified truck tyre and terrain FEA models for validation as well, paving the way for a detailed tyre model as well as further refinement of terrain modelling.

For efficiency, a rigid ring model is often used to represent a simplified tyre when simulating a quarter vehicle model. Allen et al. (2008) described a rigid ring quarter-vehicle model with force-dependent effective road profile designed in MATLAB, while Slade et al. (2009) produced a rigid ring model based on data collected from detailed FEA off-road tyre and soil models. Out-of-plane characteristic parameters of the rigid ring tyre are predicted to produce a model which reduces computing costs relative to FEA modelling. With recent advancements in commercial FEA codes and computing power, however, models have become more detailed and accurate.

In 2010, Lescoe et al. used a rigid tyre model with smooth particle hydrodynamics to simulate soil. The SPH technique offers the ability to model terrain as particles rather than solid elements, making it better suited for modelling soft soils. A more comprehensive analysis of the SPH technique in contrast to traditional FEA modelling is presented in Lescoe et al. (2011), however it is noted that further refinement of the characteristics of SPH elements is required to obtain accurate models of soft soils.

The goal of this paper is to design and construct a non-linear FEA truck tyre model that can be used to predict the rolling resistance of a particular tyre as an alternative to laboratory or field tests. Hard surfaces are used for the modelling and prediction of rolling resistance, with the possibility of future work using SPH for prediction on soft soils.

## *2.1 FEA tyre model construction*

The software used to model the tyre is the PAM-SYSTEM, comprising industry-leading code for finite element analysis. The software is used for virtual crash testing by many commercial vehicle manufacturers and recognised for its accuracy and flexibility in modelling of complex systems. For this study, the MESH, CRASH, SHOCK and VIEWER applications were primarily used to create, set up and analyse the tyre model.

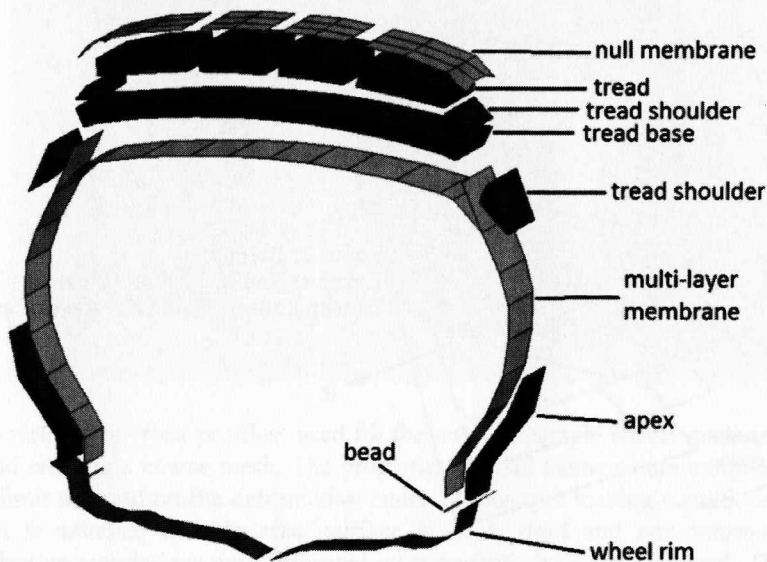
The FEA tyre model created is derived from a radial-ply aircraft tyre model developed by ESI North America, and later modified for passenger vehicles by Chang (2002). The tyre was subjected to vibration and transmissibility simulation testing with the use of a cleat-drum model, as well as demonstration of the standing wave phenomenon at high speeds using a tyre on a smooth drum model. For this paper, a full three-dimensional radial-ply truck tyre is modelled with the non-linear FEA software PAM-SHOCK.

At the base of the tyre bead, a beam element is used to represent the bead bundle in an actual tyre. This element was chosen due to the behaviour properties of the beam, which allows for accurate simulation of the bead structure. The FEA tyre construction is based on a simple set of interconnected membranes with varying properties, and solid elements to represent the tread, tread base, and apex.

The membranes are toroidal sheets of varying virtual thickness which are connected to adjacent membrane sheets by edge-to-edge connections. Additionally, the lower-most

membrane is connected to the bead material, which is then attached to the wheel rim. One of the 60 radial sections which comprise the tyres is shown in Figure 1.

**Figure 1** 1/60 radial section of the FEA tyre model (see online version for colours)



Note: The solid elements are shown in red, while the membrane elements are shown in green.

The material near the bead leading to half-way up the sidewall is layered on top of the membrane. It assists in mirroring the qualities present in that area of a tyre. It is modelled as a solid element and material properties are assigned as a Mooney-Rivlin solid. This best represents the rubber compound of a tyre and the unique loading characteristics. For this portion of the tyre, the rubber material was chosen with low Mooney-Rivlin coefficient value of C01 and high value of C10; these results in a stiffer material to better represent the effect of the carcass wrapping around the bead and up to the sidewall.

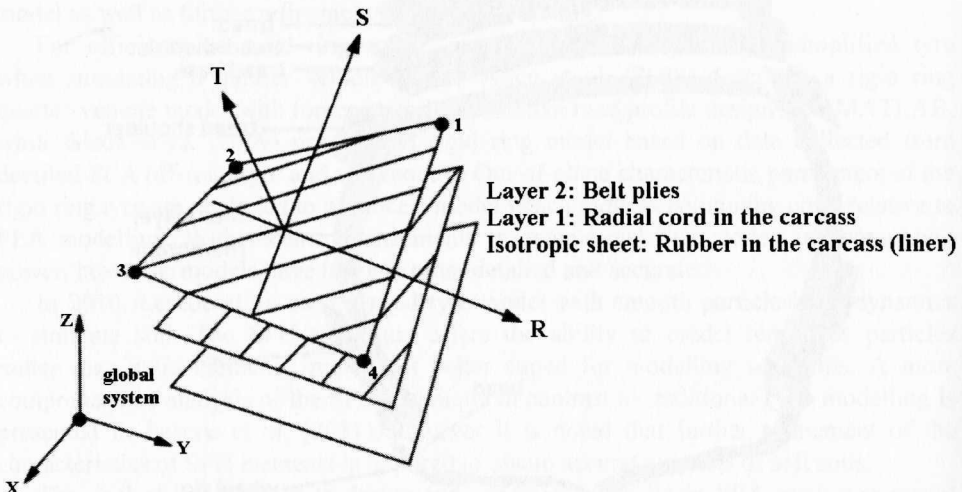
The shoulder, tread base, and tread cap are also modelled as Mooney-Rivlin solids. The shoulder elements directly adjacent to the sidewall and the tread base have stiffer characteristics while the tread has softer and more flexible material properties.

In order to best simulate a pneumatic automotive tyre, the membrane sections of the FEA model must exhibit the properties of the complex interactions between the multiple layers. Thus, the layered membrane material in PAM-CRASH is selected. This material corresponds to a linear elastic membrane material that consists of two sets of fibres, arranged at selected angles, embedded in an isotropic matrix or film material, called the parent sheet. The individual layers and the orientation of the angles of the 'fibres' are shown in Figure 2.

The lower, isotropic matrix layer represents the rubber material of the carcass of the tyre. Layer 1 represents the radial cord ply of the carcass, while layer 2 models the belt plies. It is important to note, however, that three different orientations of cords are required to model the tyre accurately. Due to the limitations of the material, the properties of the belt plies of two different directions are equivalently modelled in a direction perpendicular to the radial cord direction. The orientation of the R-axis means that a zero

cord angle is input for layer 1 to represent the radial cords. The cords running at a crown angle are smeared at a 90 degree angle from the R-axis for layer 2, however because they are only required for the area under the tread base, the material properties of layer 2 are largely negligible for the sidewalls.

**Figure 2** The three-layered membrane element



Source: ESI Group (2000)

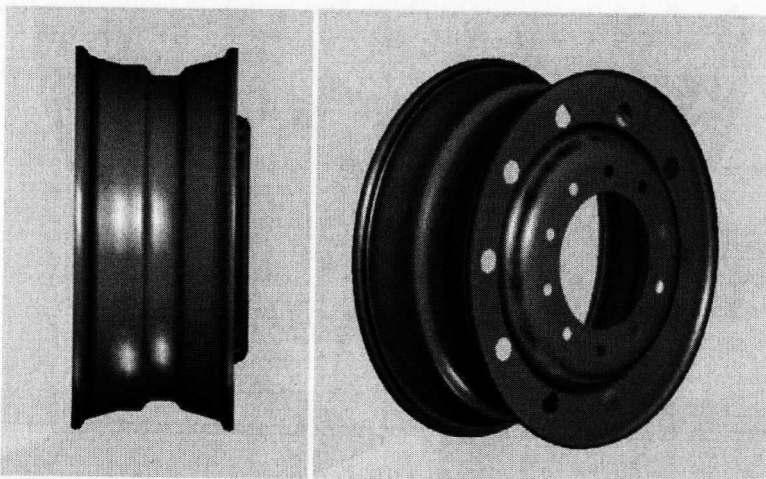
Furthermore, the membrane elements at the tread shoulders and near the bead have a considerably higher Young's modulus than those of the other membrane sections, to mimic the behaviour seen in those areas. The thickness of each membrane is varied virtually through the element card, and as with an actual tyre, it is thinnest at the sidewall. It is important to note that the hysteresis of rubber is considered only for the membrane elements, and is not simulated in the solid elements.

Once all parts consisting of the beam elements for the bead, membrane elements for the plies and cords, and solid rubber elements are assembled to create a complete section of the tyre, it is revolved around the model origin for a total of 60 individual sections. This completes a tyre model, and once all necessary connections between adjacent sections are defined, the tyre is ready for assembly with the wheel.

The FEA rim model used for this report is based on a standard set of size and contour dimensions obtained from The Tire and Rim Association. The  $8.25 \times 22.5$  in rim is shown below in Figure 3. The rim is a simple solid part with rigid body properties. The material properties were chosen as steel, which results in a rim weight of 32 kg.

It is important to make sure that contacts between the rim and tyre are defined correctly so that the tyre can inflate and maintain pressure while subject to loading and normal vehicle operations. While actual interaction between the rim and bead is complex, in the FEA model the tyre-rim interaction is modelled as a solid connection between the rim and the bead for simplicity.

**Figure 3** FEA truck tyre rim model (see online version for colours)



The test surfaces or ‘road profiles’ used for the tests are simple sheets made by plotting nodes and creating a coarse mesh. The properties of road elements are assigned as rigid body to limit the road profile deformation under various tyre loading conditions. For this report, it is assumed that the road surface is hard, rigid and non-deformable. The load-deflection simulations are performed on a perfectly smooth, flat road. The rolling resistance simulations are performed on different roads, varying from perfectly smooth to emulating the road profile of a randomly-noisy road. For all road surfaces developed, the road friction coefficient,  $\mu$ , was chosen to be 0.6, to represent the micro-level roughness of a typical road surface.

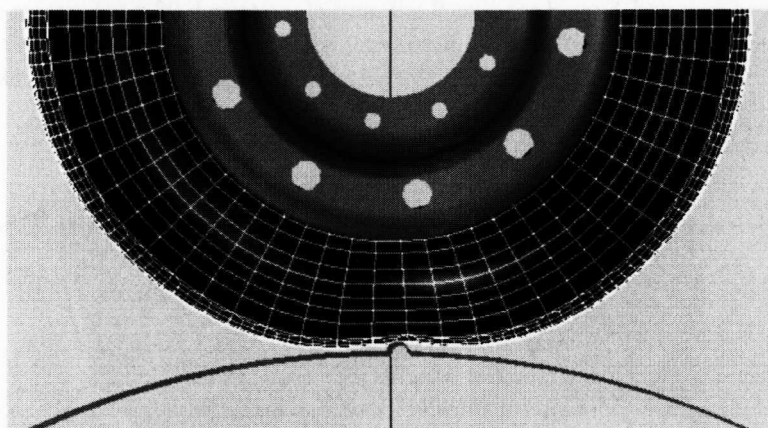
During the validation and simulations, the tyre is inflated to the desired pressure within the first few milliseconds of simulation by using a pressure force which acts on the inside face of the tyre carcass and rim.

### 3 Validation and simulation

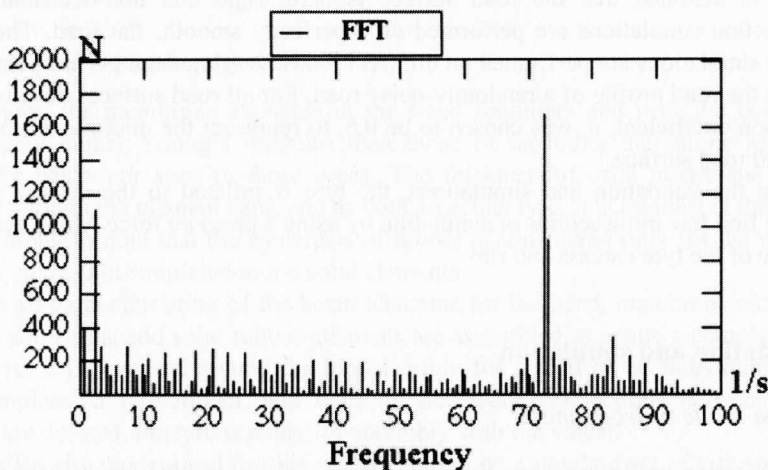
#### 3.1 First mode of frequency

The first criterion used to validate the FEA tyre model and see the results of the tyre on an uneven surface is the first mode of frequency, a test which demonstrates the dynamic response of the tyre. It is also referred to as the power spectral density and represents the different possible responses of the tyre may experience when excited with a particular input.

In order to obtain the modes of frequency, the tyre must experience vibration input; thus, an FEA model of the cleated-surface drum test rig shown in Figure 4 was created. The drum diameter is 2.5 m, while the semi-circular cleat on the drum has a height of 10 mm. An angular velocity is applied to the centre of the drum so that the tyre rolls freely at 50 km/h. The tyre spindle is fixed so that the vertical reaction force at tyre centre due to the cleat excitation can be simulated. Using the fast Fourier transform algorithm on the reaction force at the spindle, the vertical free vibration mode can be determined.

**Figure 4** Cleated-surface drum simulation (see online version for colours)

With a tyre inflation pressure of 0.759 MPa (110 psi), an equivalent spindle load of 26.7 kN, and by applying the FFT algorithm to the results, the plot shown in Figure 5 is generated.

**Figure 5** FFT results of vertical reaction force at tyre spindle

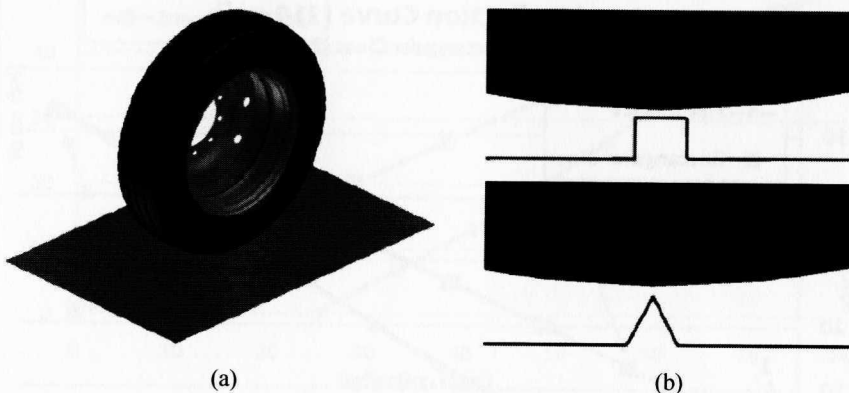
As seen in the above graph, the free vibration mode is detected at about 73 Hz, which falls within a reasonable range as discovered in previous studies (Kao, 2002; Cremers, 2005).

### 3.2 Static deflection and enveloping force

The generated FEA tyre was verified to accurately represent a general, radial-ply pneumatic truck tyre through a number of deflection tests. The FEA tyre, wheel and the rigid road are combined to form the model shown in Figure 6(a). The tyre is constrained to allow movement in the Z-direction only, and a vertical load is applied at the centre of the tyre. The deflection of the tyre centre is measured once the model has stabilised and

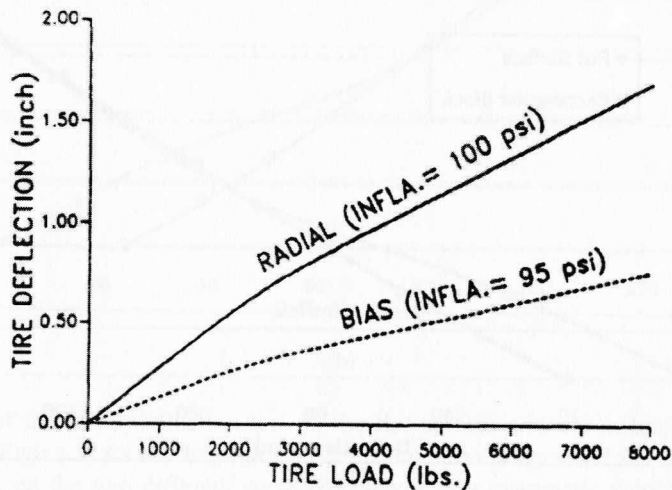
the results are compared with experimental results to determine the accuracy of the FEA model with respect to vertical stiffness. In addition to a flat surface, the deflection tests were performed on rectangular and triangular cleats, as shown in Figure 6(b), to demonstrate the enveloping characteristics of the tyre.

**Figure 6** (a) The complete FEA tyre, wheel and rigid road assembly as used for the static deflection simulations (b) The rectangular and triangular cleat profiles (see online version for colours)



The simulations conducted with regards to static deflection of a loaded tyre are similar to those outlined in SAE J2705 (2005) and can be verified by observing previous data collected regarding the subject. Figure 7 is one such example which shows the load-deflection curve of a radial and bias-ply truck tyre on a flat surface. Furthermore, experimental data collected by Alkan et al. (2011) and Kang (2008) show that at a certain point after the cleat is fully enveloped, the tyre behaves as if it were on a flat surface.

**Figure 7** Load-deflection curve of truck tyres



Source: Yap (1989)

**Figure 8** (a) The rectangular cleat load-deflection curve with a tyre inflation pressure of 110 psi  
 (b) The rectangular cleat load-deflection curve with a tyre inflation pressure of 55 psi  
 (see online version for colours)

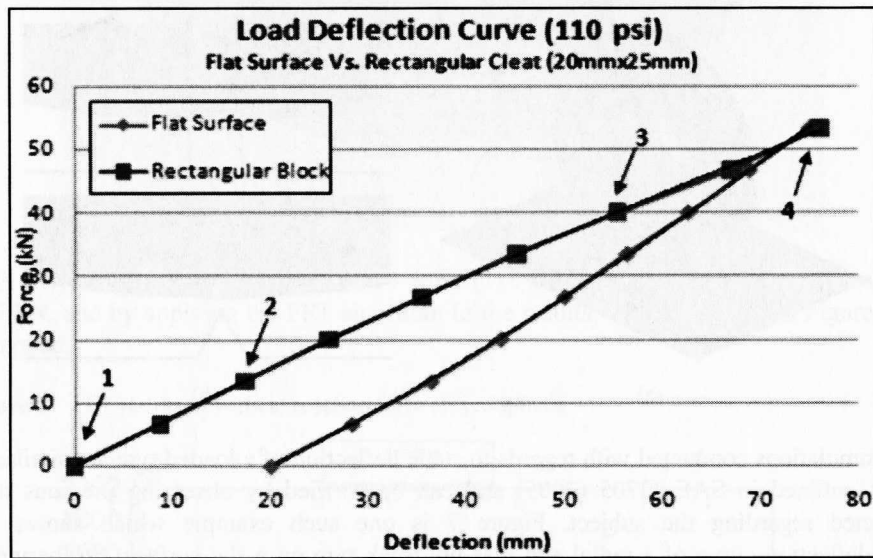


(1)

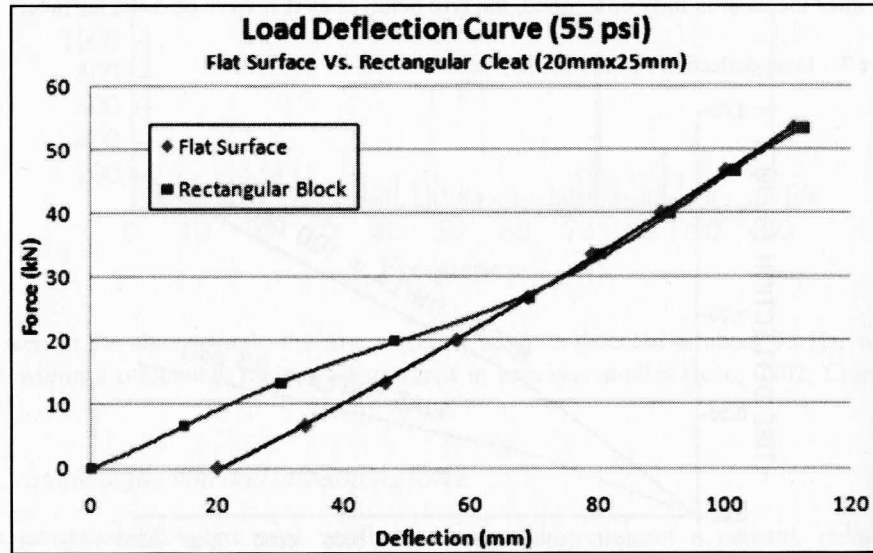
(2)

(3)

(4)

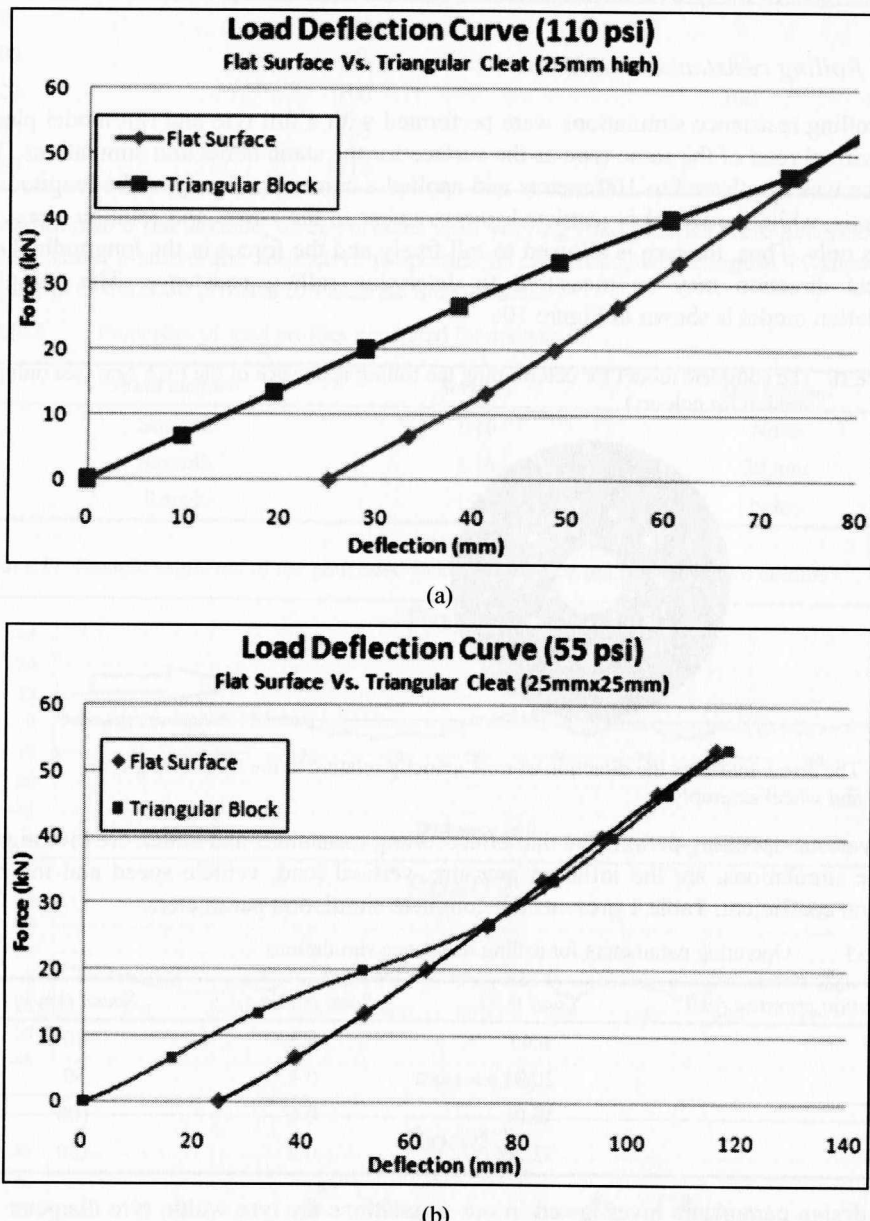


(a)



(b)

**Figure 9** (a) The triangular cleat load-deflection curve with a tyre inflation pressure of 110 psi  
 (b) The triangular cleat load-deflection curve with a tyre inflation pressure of 55 psi  
 (see online version for colours)



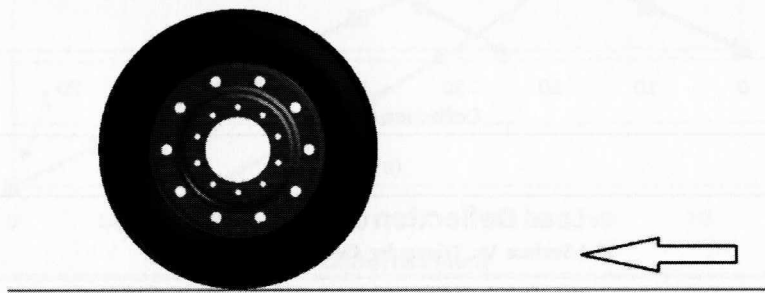
The results of the static deflection test on the flat surface and the rectangular cleat are presented in Figure 8. As can be seen from the simulation images and the curves derived, the FEA tyre on the two different surfaces behaves as a pneumatic vehicle tyre would, converging at the point of full envelopment. Similarly, the triangular cleat simulation results present a curve which closely models the expected behaviour of the FEA tyre, as shown in Figure 9.

It is of note that the flat surface deflection curves are shifted by 20 mm and 25 mm for the rectangular and triangular cleats, respectively, to account for the higher initial displacement of the tyre on the cleat tests.

### 3.3 Rolling resistance simulations

The rolling resistance simulations were performed with a full tyre and rim model placed on a virtual road of the same type as the surface for the static deflection simulations. The surface was lengthened to 100 metres and applied a constant velocity in the longitudinal tyre axis, while the wheel is restricted to movement in the z-axis and rotation along the y-axis only. Thus, the tyre is allowed to roll freely and the forces in the longitudinal and vertical direction may be measured to determine rolling resistance. The complete simulation model is shown in Figure 10.

**Figure 10** The complete model for determining the rolling resistance of the FEA tyre (see online version for colours)



Note: The arrow indicates the direction of road velocity relative to the free-rolling tyre and wheel assembly.

The various operating parameters that effect rolling resistance, and which are investigated in the simulations, are the inflation pressure, vertical load, vehicle speed and the road friction coefficient. Table 1 presents the complete simulation parameters.

**Table 1** Operating parameters for rolling resistance simulations

Inflation pressure (psi)	Load (kN)	Road friction $\mu$	Speed (km/h)
27.5	6.67	0.2	10
55	20.01	0.4	50
110	40.01	0.6	100
165	53.36	0.8	150

The design parameters investigated in our simulations are tyre width, tyre diameter and tread depth. Table 2 shows the factors by which the original design was varied to observe their effect. It is also important to note that the tyre validation simulations were performed on the modified tyres and both static and dynamic response was shown to be generally consistent.

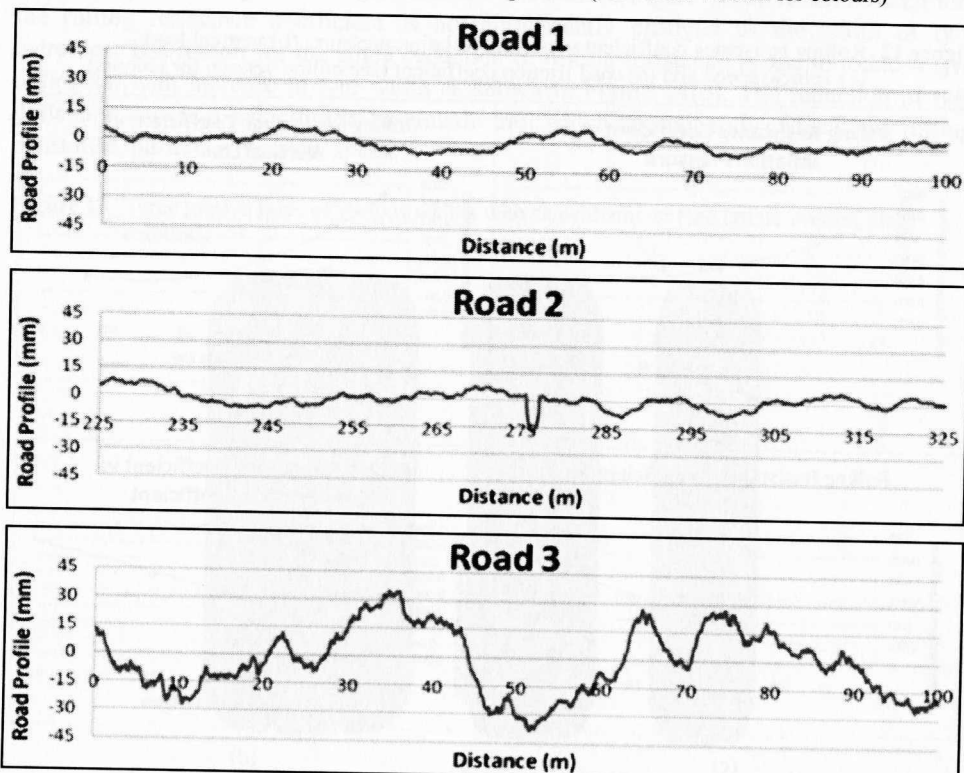
**Table 2** Design parameters for rolling resistance simulations

Tyre width (%)	Tyre diameter (%)	Tread depth (%)
80	80	0
100	90	42
120	100	100
140	105	
160	110	

In addition to a flat surface, three surfaces with varying road profiles were generated and tested. Table 3 shows the respective properties of each road, while Figure 11 shows the segments of the road profiles to visualise the surfaces:

**Table 3** Properties of road profiles generated for analysis

#	Road surface	Severity	Ditch/bump
1	Smooth	1.16	None
2	Smooth	1.16	20 mm
3	Rough	15.6	None

**Figure 11** Sample segments of the generated road profiles (see online version for colours)

The slip and camber angle simulations were performed on a perfectly flat surface. Table 4 shows the set of angles simulated in FEA model.

**Table 4** Slip and camber angles simulated in the FEA model

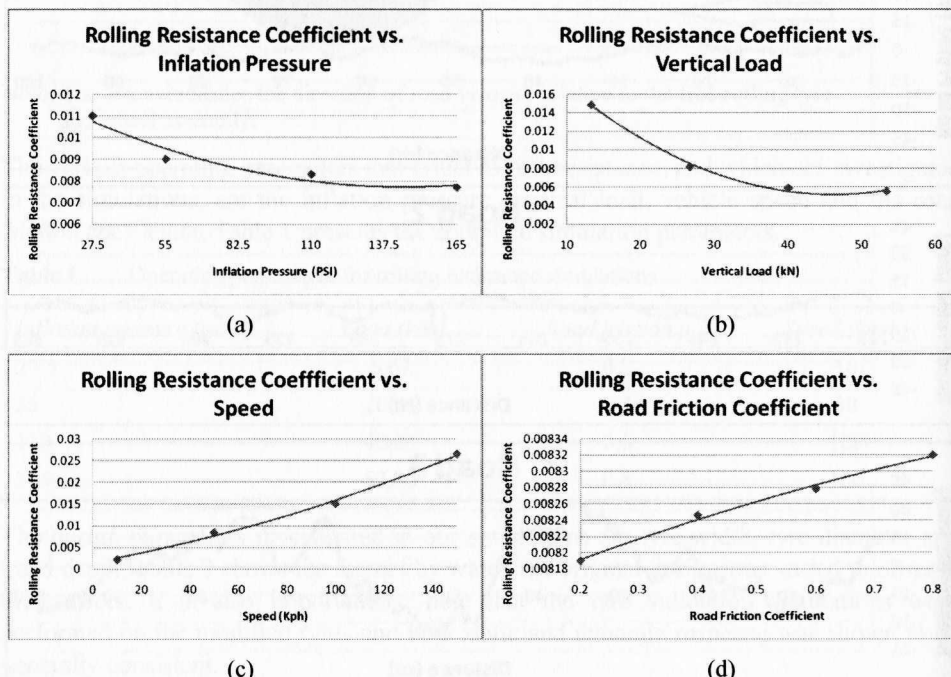
Slip angle (degrees)	Camber angle (degrees)
0	0
±2	±1.5
±4	±3.0
±6	
±8	
±10	
±12	

## 4 Results and discussion

### 4.1 Influence of design and operating parameters on rolling resistance

The results presented in Figure 12 show the individual operating parameters and their influence on the rolling resistance coefficient. Each parameter is varied individually, and each has a default control value as follows: inflation pressure of 110 psi, vertical load of 26.68 kN, road friction coefficient of  $\mu = 0.6$  and vehicle speed of 100 km/h.

**Figure 12** Rolling resistance coefficient versus (a) inflation pressure, (b) vertical load, (c) vehicle speed and (d) road friction coefficient (see online version for colours)



The compiled results of the rolling resistance simulations provide a clear picture regarding the effect of the four observed operating parameters. As expected, the inflation pressure has an inverse curve, demonstrating that higher inflation pressures tend to reduce the overall rolling resistance of the tyre. In contrast, the influence of speed on the rolling resistance, and thus the rolling resistance coefficient, shows an increasing exponential curve. These correlate well with results presented in Wong (2008) and Dukkipati et al. (2008).

The vertical load curve shows that as load increases, the rolling resistance coefficient decreases. This may be counter-intuitive, but the data shows that rolling resistance force ( $F_x$ ) increases as load ( $F_z$ ) increases. However, a significant increase in the vertical load applied to the tyre does not result in a proportional increase in the rolling resistance force. Thus, the rolling resistance coefficient curve shows a decreasing relationship with the vertical tyre load.

The road friction coefficient represents the micro-level roughness of the road, and determines the interaction of the road-tyre contact. Simulations of the four selected values, ranging from 0.2 to 0.8, show that the rolling resistance increases with the road friction coefficient, however the effect tends to taper slightly as the values increase. Once again, the results are consistent with existing works which show that the micro-level road texture has a positive correlation with the rolling resistance coefficient.

The effect of tyre width between the range of 0.8 and 1.6 times of original width (Figure 13) on rolling resistance coefficient is shown in Figure 14(a). It can be seen that the rolling resistance coefficient is not significantly changed as the width of tyre increases. The reason for the slight reduction of rolling resistance is due to reduced tyre deflection with increase in tyre width as shown in Figure 14(b). The reduction of tyre deflection causes a reduction in pneumatic trail which consequently reduces the rolling resistance, particularly at low speeds.

**Figure 13** Three groove tyres of various widths with same diameter (see online version for colours)

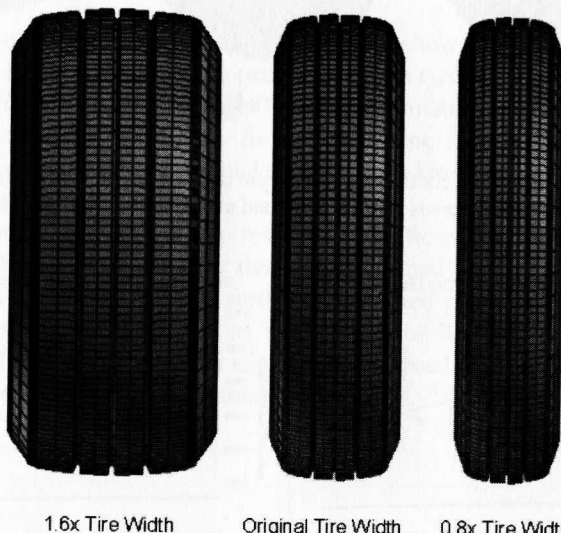
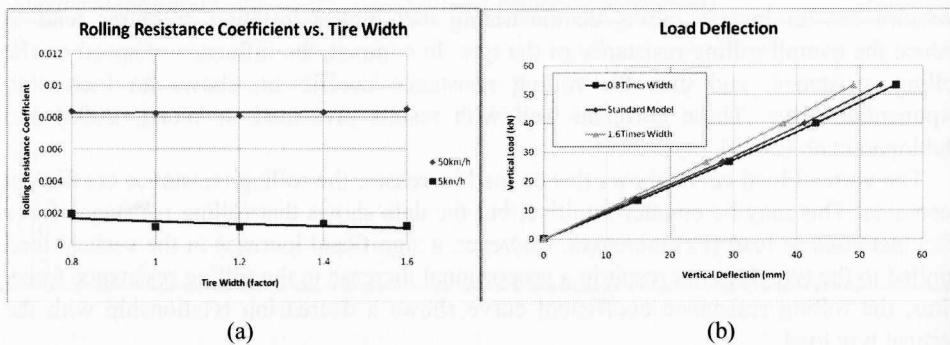


**Figure 14** (a) Rolling resistance coefficient versus tyre width at 50 and 5 km/h (b) Load deflection versus tyre vertical load at various tyre widths (see online version for colours)



The tyre diameter has been also changed between 0.9 and 1.1 as shown in Figure 15. As the tyre diameter increases the rolling resistance is reduced at the same constant vertical load and inflation pressure. This is due to the reduced tyre deflection as the diameter increases shown in Figure 16(b).

**Figure 15** Tyres with same width and varying diameter (see online version for colours)

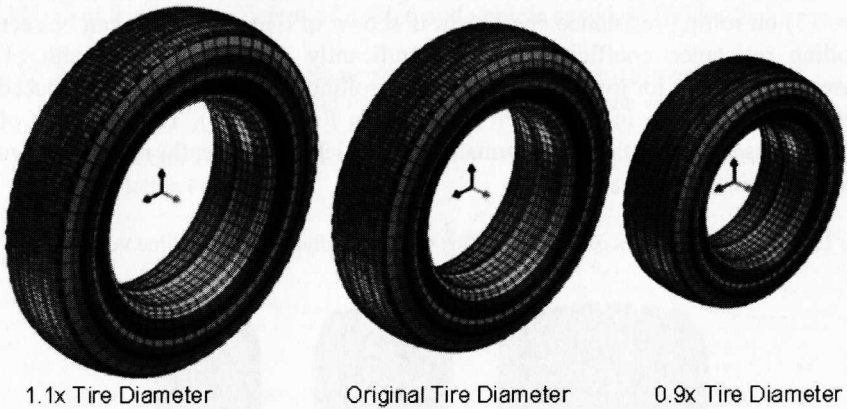
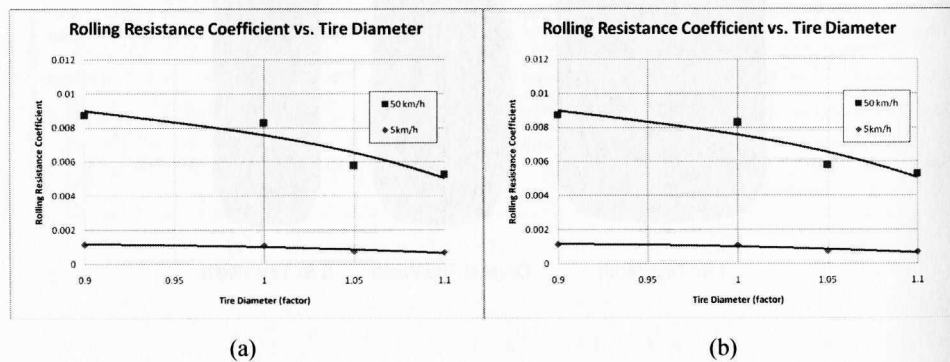


**Figure 16** (a) Rolling resistance coefficient versus tyre diameter at 50 and 5 km/h  
(b) Load deflection versus tyre vertical load at various tyre diameters (see online version for colours)

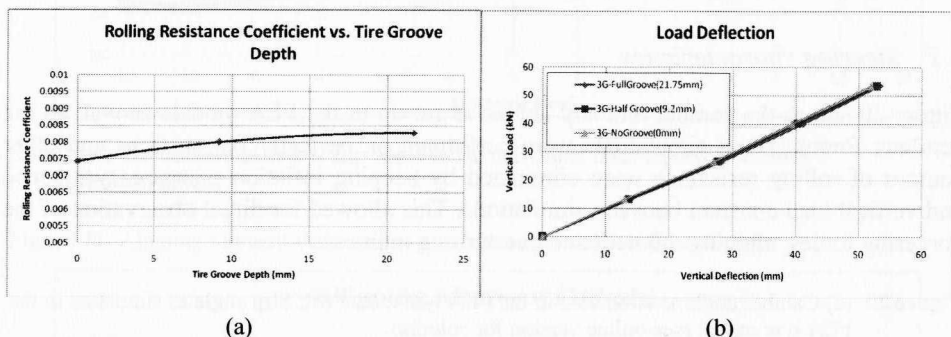


The groove depth results show that deeper grooves tend to increase the rolling resistance produced by the tyre due to increased flexibility in the tread area, causing more hysteresis. Figure 17 shows FEA models with various groove depths while Figure 18 shows the results of the simulation.

**Figure 17** Three groove tyre with various groove depths

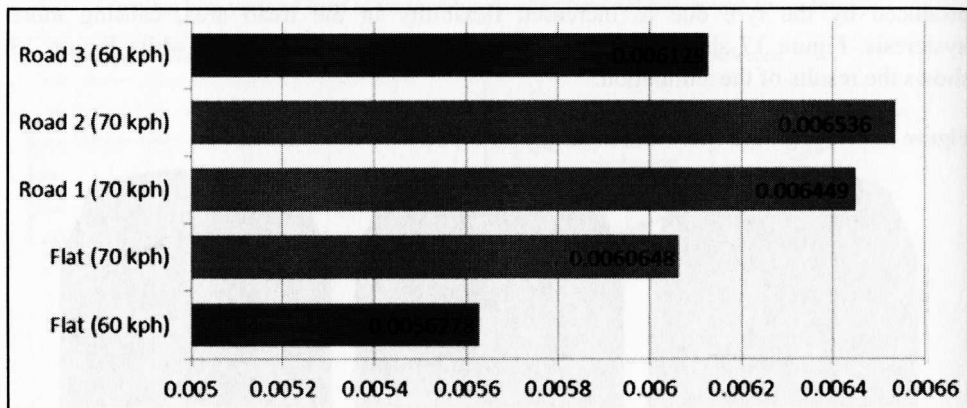


**Figure 18** (a) Rolling resistance coefficient versus groove depth (b) Tyre vertical deflection versus load (see online version for colours)



For the three road surfaces generated, the results show that road roughness has a significant effect on the overall rolling resistance of the tyre. Figure 19 presents the three road surface simulation results, averaged over ten simulations for each road, as well as the results obtained on a flat surface for corresponding speeds. Note that simulations shown in red were performed at a vehicle speed of 60 km/h, while those shown in blue were performed at 70 km/h.

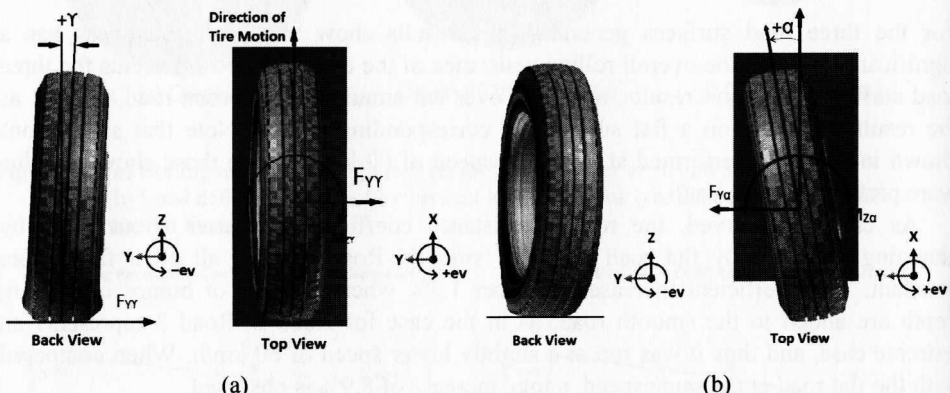
As can be observed, the rolling resistance coefficient increases about 7.8% by changing the perfectly flat road with the 'smooth' Road 1 while all other factors are constant. The coefficient increases a further 1.3% when potholes or bumps of 20 mm depth are added to the smooth road, as in the case for Road 2. Road 3 represents an extreme case, and thus it was run at a slightly lower speed of 60 km/h. When compared with the flat road at the same speed, a total increase of 8.9% is observed.

**Figure 19** Rolling resistance over various road surfaces (see online version for colours)

Notes: Tyre velocity for Roads 1 and 2 is 70 kph (in blue). Tyre velocity for Road 3 is 60 kph (in red). Road 3 represents an extreme case due to large variations in surface texture. Tyre inflation pressure is 110 psi; tyre load is 26.68 kN; road friction coefficient  $\mu = 0.6$ .

#### 4.2 Steering characteristics

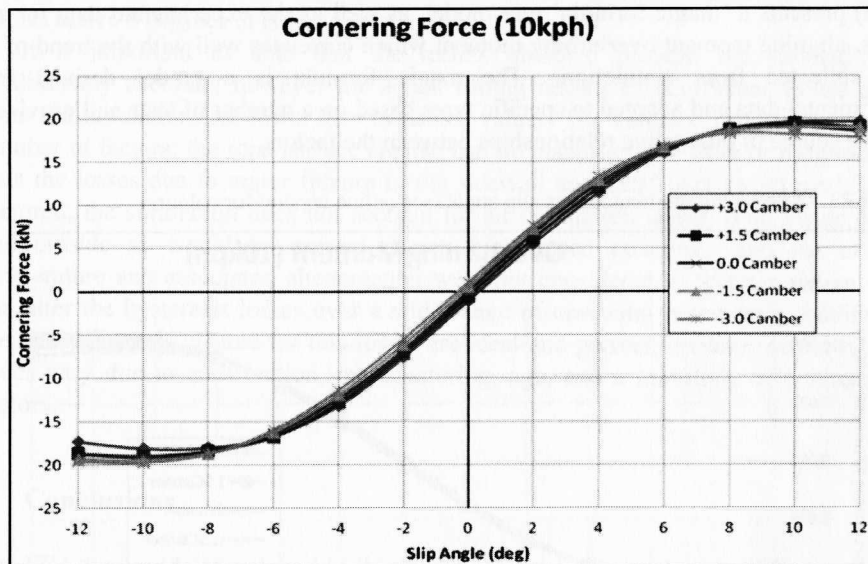
Figure 20 shows the camber and slip angles as set up in the FEA models as well as the resultant forces. These simulations were performed on perfectly flat surfaces and other sources of rolling resistance were eliminated by keeping inflation pressure, tyre speed and vertical load constant between simulations. This allowed for direct observation of the cornering forces, aligning moment and overturning moment.

**Figure 20** (a) Camber angle as simulated in the FEA tyre model (b): Slip angle as simulated in the FEA tyre model (see online version for colours)

The predicted cornering forces with respect to different slip angles up to 12 degrees are plotted in Figure 21 and compared with actual measurements (El-Gindy and Chae, 2001). The applied vertical loads were 17.79 kN (4,000 lbs), 26.69 kN (6,000 lbs), and 35.59 kN (8,000 lbs) and the speed was 10 km/h. The predicted cornering forces are in good agreement with the measurements especially for the two cases of the lower vertical loads,

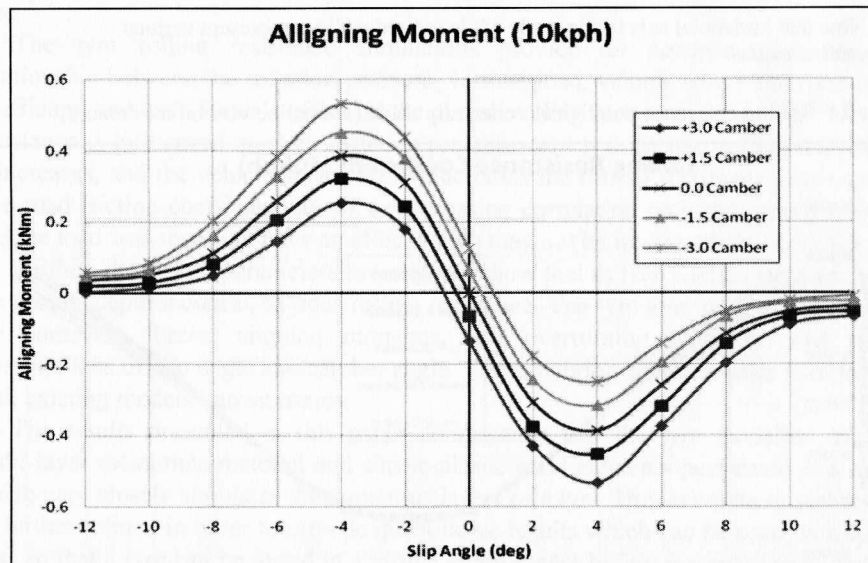
17.79 kN and 26.69 kN. Similarly, the aligning moment and overturning moment are plotted in Figures 22 and 23, respectively.

**Figure 21** Cornering force versus slip angle (see online version for colours)



Note: Note that horizontal axis is slip angle while individual lines represent various camber angles.

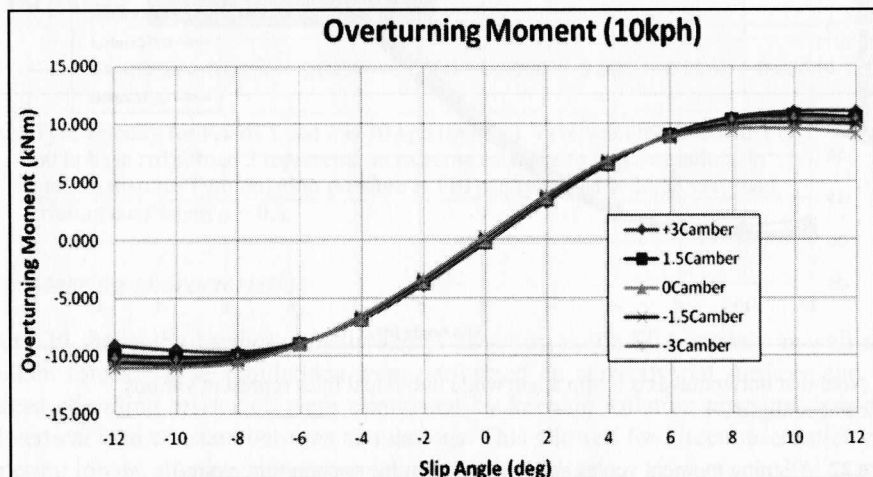
**Figure 22** Aligning moment versus slip angle (see online version for colours)



Note: Note that horizontal axis is slip angle while individual lines represent various camber angles.

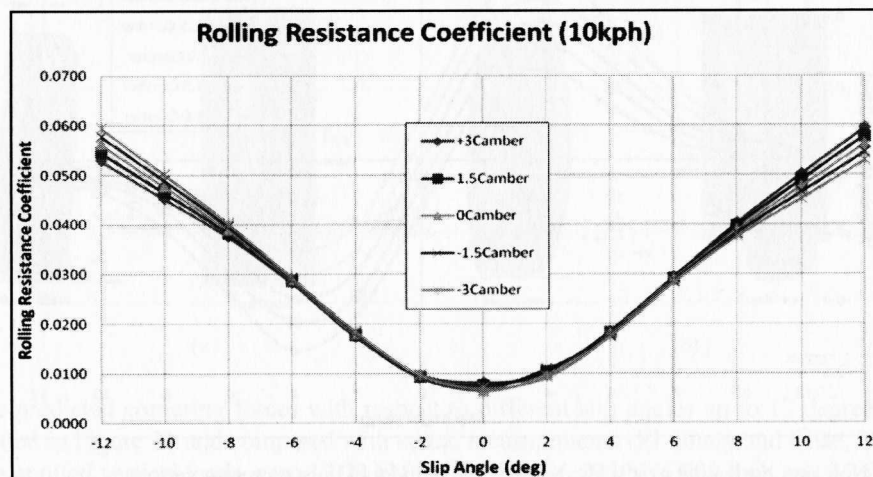
The side, or cornering force, varies minimally over the various camber angles simulated and shows heavy influence of slip angle. It is apparent that the camber angle has an influence on both aligning and overturning moments, but is more prominent in the production of aligning moment within the range of tested camber and slip angles. Pacejka (2006) presents a ‘magic formula’ tyre model, as well as the experimental data for side forces, aligning moment overturning moment which correlates well with the trend of the data collected from simulations. The magic formula is a model derived from experimental data and adapted to specific tyres based on a number of tests and provides a reliable source of qualitative relationships between the factors.

**Figure 23** Overturning moment versus slip angle (see online version for colours)



Note: Note that horizontal axis is slip angle while individual lines represent various camber angles.

**Figure 24** Rolling resistance coefficient versus slip angle (see online version for colours)



Note: Note that horizontal axis is slip angle while individual lines represent various camber angles.

Figure 24 presents the rolling resistance simulation results with slip and camber angles of varying amounts. As can be seen, the slip angle heavily influences the rolling resistance due to the large deformations produced while the tyre turns. The effect of camber is not very prominent at low slip angles; however there is some noticeable influence at slip angles above 6 degrees in either direction.

It is important to note that the results obtained through the simulations are qualitatively accurate; however the actual rolling resistance coefficient values derived from the simulations are lower than measured values. The variation can be attributed to a number of factors: the road surface created had no macro-level texture or roughness, and thus the losses due to major flexure in the sidewall and tread over rough roads are not factored; the simulation does not account for air circulation losses, both inside the tyre and outside as would be present during high speed operation; and the effect of temperature and associated phenomenon were not considered in this simulation, which can alter the hysteresis losses over a wide range of operating parameters. Additionally, the tyre and roads created for this report are ideal and perfect; however actual tyres and roads vary due to construction, manufacturing, age, and a multitude of environmental factors.

## 5 Conclusions

The FEA tyre model developed in this report shows good correlation with respect to the qualitative effects of various operating parameters on the rolling resistance coefficient of a modern radial heavy truck tyre. Through the testing of static deflection, cleat envelopment characteristics, and the power spectral density (modes of operation) the tyre has been verified to be accurate in modelling the behaviour of a radial pneumatic truck tyre.

The tyre rolling resistance simulations provide an accurate cause-and-effect relationship between the inflation pressure, vertical load, vehicle speed and road friction coefficient and each factor's effect on the overall rolling resistance of a tyre. The rolling resistance is influenced most by inflation pressure, which decreases rolling resistance as it increases, and the vehicle speed, which increases the rolling resistance as it increases. The road friction coefficient shows an increasing correlation with the rolling resistance and the load was shown to have an effect which may not be intuitive but is accurate.

Further, the design parameters investigated show that as tyre width, tyre diameter and the groove depth increase, so does rolling resistance. The tyre also accurately reproduces the cornering forces, aligning moments, and overturning moments with various combinations of slip angle and camber angle. These steering characteristics correlate well with existing models known trends.

The results presented in this paper demonstrate that the tyre modelled using the multi-layer membrane material and elastic-plastic solid elements performed in a manner which very closely simulates the numerous layers of a tyre. However, the model needs to be further refined in order to provide quantitative results which can be used on a specific tyre, so that a tyre can be tested in a virtual environment before manufacturing, reducing the costs of development and prototyping. Effects such as air circulation, influence of temperature and the associated hysteresis losses, and the effect of terrain on the rolling resistance remain topics for further investigation.

## Acknowledgements

The authors would like to express their appreciation to Mr. Stefan Edlund of Volvo Group Trucks Technology for his continuous technical help during the course of this study.

## References

- Alkan, V., Karamihas, S.M. and Anlas, G. (2011) 'Finite element modeling of static tire enveloping characteristics', *International Journal of Automotive Technology*, Vol. 12, No. 4, pp.529–535.
- Allen, J., II, El-Gindy, M. and Koudela, K. (2008) 'Development of rigid ring quarter-vehicle model with an advanced road profile for durability and ride comfort predictions', *Proceedings of DETC'08, 2008 ASME International Design Engineering Technical Conference*, Paper No. DETC2008-49031, 3–6 August, New York, NY.
- Allen, J., II, Shoffner, B., El-Gindy, M., Trivedi, M., Johansson, I. and Öijer, F. (2007) 'Prediction of tire-terrain interaction using finite element analysis model', *2007 ASME International Design Engineering Conferences, 9th International Conference on Advanced Vehicle and Tire Technologies (AVTT)*, 4–7 September, Las Vegas, Nevada, pp.1–12.
- Chae, S., El-Gindy, M., Allen, J., II, Trivedi, M., Johansson, I. and Öijer, F. (2006) 'Dynamic response predictions of quarter vehicle models using a finite element analysis and rigid ring truck tire models', *2006 ASME International Mechanical Engineering Congress, 8th Symposium on Advanced Vehicles Technologies*, 5–11 November, Chicago, IL, pp.1–10.
- Chang, Y.P. (2002) 'Nonlinear rotating tire modeling for transient response simulations', PhD thesis, The Pennsylvania State University, University Park, PA, USA.
- Cremers, R. (2005) 'Investigating dynamic tyre model behaviour', PhD thesis, Eindhoven University of Technology, Eindhoven, The Netherlands.
- Dukkipati, R.V., Pang, J., Qatu, M.S., Sheng, G. and Shuguang, Z. (2008) *Road Vehicle Dynamics*, 852p, SAE International, Warrendale.
- El-Gindy, M. and Chae, S. (2001) 'Examination of steering wheel lateral saturation of DaimlerChrysler transport trucks', PTI Final Report, No. PTI-2001-21, Pennsylvania Transportation Institute (PTI), The Penn State University.
- ESI Group (2008) *Explicit Solver Notes Manual*, ESI Group, Paris, France.
- Fitch, J.W. (1994) *Motor Truck Engineering Handbook*, 464p, Society of Automotive Engineers, Warrendale.
- ISO 28580:2009 (2009) 'Passenger car, truck and bus tyres – methods of measuring rolling resistance – single point test and correlation of measurement results', International Organization for Standardization.
- Kang, N. (2009) 'Prediction of tire natural frequency with consideration of the enveloping property', *International Journal of Automotive Technology*, Vol. 10, No. 1, pp.65–71.
- Kao, B.G. (2002) 'Tire vibration modes and tire stiffness', *Tire Science and Technology*, TSTCA, Vol. 30, No. 3, pp.136–155.
- Lescoe, R., El-Gindy, M., Koudela, K., Trivedi, M., Johansson, I. and Öijer, F. (2010) 'Off-road tire-soil modeling using FEA and smooth particle hydrodynamics techniques', *DETC'10, 2010 ASME International Design Engineering Technical Conference*, 12–16 August, Montreal, Canada.
- Lescoe, R., El-Gindy, M., Trivedi, M., Johansson, I. and Öijer, F. (2011) 'Off-road tire-soil modeling using FEA and smooth particle hydrodynamics techniques', *DETC'11, 2011 ASME International Design Engineering Technical Conference*, 31 August to 5 September, Montreal, Canada.
- Pacejka, H.B. (2006) *Tire and Vehicle Dynamics*, 642p, SAE International, Warrendale.

- Rakah, H., Lucic I., Demachi, S.H., Setti, J.R. and Aerde, M.V. (2001) 'Vehicle dynamics model for predicting maximum truck acceleration levels', *Journal of Transportation Engineering*, Vol. 127, pp.418-425, ASCE, New York, NY.
- SAE J1269 (2000) 'Rolling resistance measurement procedure for passenger car, light truck, and highway truck and bus tires', SAE International.
- SAE J2705 (2005) 'Tire quasi-static envelopment of triangular/step cleats test', SAE International.
- Slade, J., El-Gindy, M., Lescoe, R., Öijer, F., Trivedi, M. and Johansson, I. (2009) '3-D FEA truck tire-soft terrain modeling', *DETC'09, 2009 ASME International Design Engineering Technical Conference*, 30 August to 2 September, San Diego, CA.
- Wong, J.Y. (2008) *Theory of Ground Vehicles*, 560p, John Wiley and Sons, Ottawa.
- Yap, P. (1989) 'Truck tire types and road contact pressure', Paper, *Second International Symposium on Heavy Vehicle Weights and Dimensions*, Kelowna, British Columbia.